

Title	Anomalous magnetoresistance and hidden spin canting in (DIETSe) ₂ MCl ₄ (M=Fe, Ga)
Author(s)	Maesato, Mitsuhiro; Kawashima, Tomohito; Saito, Gunzi; Shirahata, Takashi; Kibune, Megumi; Imakubo, Tatsuro
Citation	Physical Review B (2013), 87(8)
Issue Date	2013-02
URL	http://hdl.handle.net/2433/172073
Right	©2013 American Physical Society
Type	Journal Article
Textversion	publisher



Anomalous magnetoresistance and hidden spin canting in $(\text{DIETSe})_2\text{MCl}_4$ ($M = \text{Fe}, \text{Ga}$)

Mitsuhiko Maesato,^{*} Tomohito Kawashima, and Gunzi Saito[†]

Division of Chemistry, Graduate School of Science, Kyoto University, Kitashirakawa Oiwake-cho, Sakyo-ku, Kyoto, 606-8502, Japan

Takashi Shirahata,[‡] Megumi Kibune, and Tatsuro Imakubo[§]

Imakubo Initiative Research Unit, RIKEN, 2-1 Hirosawa, Wako, Saitama 351-0198, Japan

(Received 22 November 2012; published 14 February 2013)

The quasi-one-dimensional (Q1D) molecular conductors $(\text{DIETSe})_2\text{MCl}_4$ [$M = \text{Fe}, \text{Ga}$] undergo a spin density wave (SDW) transition below 12 K. The SDW ground state is suppressed by applying high pressure, recovering the Q1D Fermi surface which is confirmed by the appearance of Lebed resonance in the angle-dependent magnetoresistance (MR). Above the critical pressure of SDW, MR shows kink structures at high magnetic fields, reminiscent of field-induced spin density wave (FISDW) transition in both salts. The π - d hybrid $(\text{DIETSe})_2\text{FeCl}_4$ also exhibits an antiferromagnetic (AF) transition of d -electron spins at 2.5 K, below which the spin-flop-induced positive large MR are observed. The change in the interlayer MR reaches 130% at 10.5 kbar. The resistance anomalies associated with spin flop are also observed in the angle-dependent MR at low magnetic fields below 5 T, associated with clear hysteresis. A polar plot of these anomalies reveals the presence of hidden spin canting. Two magnetic easy axes of d -electron spins are found to be tilted ± 16 degrees from the b axis towards the c axis. The interplay between the SDW instability of Q1D π electrons and the local moments of AF d -electron spins is considered as the origin of the anomalous transport behaviors.

DOI: [10.1103/PhysRevB.87.085117](https://doi.org/10.1103/PhysRevB.87.085117)

PACS number(s): 75.30.Fv, 75.47.-m

I. INTRODUCTION

Interplay between itinerant electrons and localized spins is one of the central issues in solid state physics. The influence of magnetic moments on the various electronic states such as Mott-Hubbard, charge ordered, spin-Peierls, charge density wave (CDW), spin density wave (SDW), and superconducting states is of particular interest. Molecular conductors are ideal systems for the investigation of the strongly correlated low dimensional electrons, since they normally have a simple and highly anisotropic electronic structure with a narrow band. In order to investigate the possible influence of magnetic moments on the ground states of molecular conductors and try to manipulate both spin and charge degrees of freedom simultaneously, a number of π - d hybrid magnetic conductors have been developed and examined.¹⁻⁴ For example, the magnetic-field-induced superconductivity was discovered in the layered conductor λ -(BETS)₂FeCl₄,⁵ and the highly one-dimensional semiconductor based on phthalocyanine showed giant negative magnetoresistance (MR),⁶ representing significant π - d interaction.

In this paper, we focus our attention on the quasi-one-dimensional (Q1D) system. As is well known, the Q1D metal is unstable against the $2k_F$ periodic potential and forms a CDW or an SDW state as a consequence of electron-phonon or electron-electron interactions, respectively, where k_F is the Fermi wave vector. The SDW was first theoretically discussed by Overhauser^{7,8} and then extensively studied experimentally, for example, in molecular conductors such as TMTSF salts, where TMTSF denotes tetramethyl-tetraselenafulvalene. TMTSF salts have attracted much attention because of their rich variety of electronic states, such as SDW, superconducting, and field-induced spin density wave (FISDW) states, depending on temperature, pressure, and magnetic field.⁹ Moreover, in the salts with noncentrosymmetric tetrahedral anions, a metal-insulator transition can also be induced by

anion ordering. It is of great interest to investigate possible influence of magnetic moments on these electronic states of the Q1D system.

It is notable that the SDW instability can couple to the local moments in the Q1D π - d system, because the $2k_F$ periodic internal field would induce an SDW state. Some Q1D π - d conductors based on tetrathiafulvalene (TTF) derivatives were reported to show anomalous MR associated with spin-flop transition of d -electron spins,^{2,10-16} suggesting coupling of the electronic instability of low dimensional π electrons with local moments. However, most of them are semiconductors well above the Néel temperature of d -electron spins, thereby possessing low carrier density. In order to examine the interplay between the itinerant electrons and local magnetic moments, the system near the border of a metal-insulator transition should be a good candidate since its electronic state is highly susceptible to external stimuli.

In 2006, Shirahata and Imakubo *et al.* synthesized new Q1D π - d conductors $(\text{DIETSe})_2\text{MCl}_4$ [$M = \text{Fe}, \text{Ga}$], where DIETSe represents diiodo(ethylenedithio)tetraselenafulvalene.¹⁷ These salts are isostructural to each other having nearly the same lattice parameters and band structures. The Fe salt possesses localized d -electron spins of high spin state ($S = 5/2$), while the Ga salt does not. Therefore, comparing the Ga salt with the Fe salt, one can elucidate the inherent nature of π electrons as well as the role of d -electron spins. The DIETSe molecules are stacking along the a -axis direction in a head-to-tail fashion as shown in Fig. 1(a). The transfer energy along the stacking direction was calculated to be about one order of magnitude larger than those along the transverse c -axis direction, giving rise to the Q1D Fermi surface as shown in Fig. 1(b). The DIETSe molecule has iodine atoms at the terminal which play an important role in the interaction with counter anions through an “iodine bond.” We note that the tetrahedral anions are ordered even

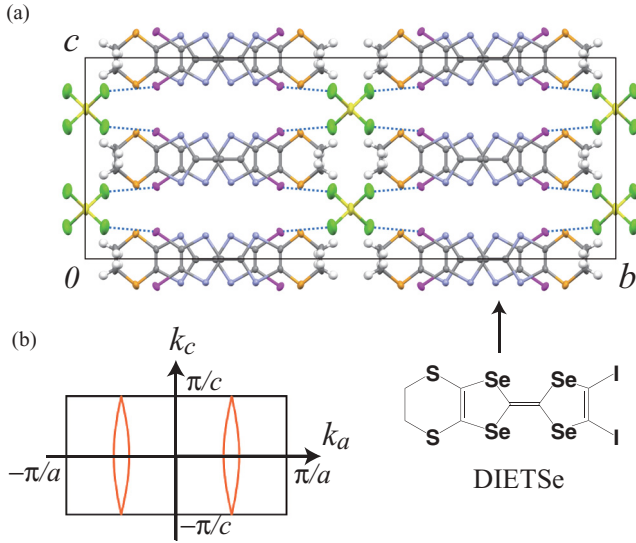


FIG. 1. (Color online) (a) Crystal structure of $(\text{DIETSe})_2\text{MCl}_4$ [$M = \text{Fe}, \text{Ga}$] viewed along the a axis (gray: C, white: H, orange: S, blue: Se, purple: I, yellow: M, green: Cl). The dotted lines indicate iodine bonds. (b) Calculated Fermi surface in the k_a - k_c plane.

at room temperature due to the iodine bond. The DIETSe molecule also involves heavy Se atoms in the inner TSF skeleton, which effectively increases the intermolecular interaction and therefore bandwidth, leading to a highly conducting state down to low temperature.¹⁷ Actually both salts are metallic down to about 12 K, below which resistance increases with decreasing temperature at ambient pressure.¹⁷ The semiconducting behavior below 12 K has been attributed to the SDW transition due to nesting instability of the Q1D Fermi surface.¹⁸ The ⁷⁷Se NMR measurement of the Ga salt revealed a peak in the relaxation rate T_1^{-1} around 7 K, accompanied by significant broadening of the spectra below the temperature, indicating the emergence of an inhomogeneous local field.¹⁸ The shape of the spectra in the magnetically ordered state is characteristic of an incommensurate SDW (ICSDW). The magnetic susceptibility measurements revealed an antiferromagnetic (AF) transition of d -electron spins at about 2.5 K in $(\text{DIETSe})_2\text{FeCl}_4$.¹⁷ Therefore the SDW coexists with the AF order in the ground state, where anomalous magnetotransport behaviors have been observed.^{19,20} Remarkably, $(\text{DIETSe})_2\text{FeCl}_4$ shows spin-flop-induced steep positive MR and nonvolatile magnetoresistive memory due to the interplay between the SDW instability of Q1D π electrons and the local moments of AF d -electron spins.²⁰

In order to precisely investigate the influence of magnetic moments on the Q1D electrons having an SDW instability and clarify the electronic states at low temperature, we have performed detailed studies of magnetic-field, pressure, and angular dependence of MR in the Q1D molecular conductor $(\text{DIETSe})_2\text{MCl}_4$ [$M = \text{Fe}, \text{Ga}$].

II. EXPERIMENTAL

Single crystals of $(\text{DIETSe})_2\text{MCl}_4$ [$M = \text{Fe}, \text{Ga}$] were synthesized by conventional electrochemical oxidation method.¹⁷

Typical shape of the crystals is an elongated plate, elongated along the most conducting a -axis direction. Interlayer resistivity was measured by a conventional four-probe method with direct current applied along the least conducting b -axis direction. Hydrostatic pressure was applied using a clamp-type small BeCu pressure cell. Daphne 7373 oil was used as a liquid pressure-transmitting medium. Pressure at low temperature was estimated by considering the pressure loss during cooling.²¹ The pressure cell was placed on a single-axis rotator in order to measure the angular dependence of MR. A solenoid-type superconducting magnet was used to generate high magnetic field up to 12 T.

III. RESULTS AND DISCUSSION

The ratio of electrical conductivity σ_a/σ_b of $(\text{DIETSe})_2\text{MCl}_4$ [$M = \text{Fe}, \text{Ga}$] is about 10^4 at room temperature and ambient pressure, where σ_a and σ_b represent the electrical conductivity along the a - and b -axis directions, respectively.²⁰ It indicates that these salts are highly anisotropic conductors.

Temperature dependence of interlayer resistivity of $(\text{DIETSe})_2\text{MCl}_4$ [$M = \text{Fe}, \text{Ga}$] under hydrostatic pressures are shown in Figs. 2(a) and 2(b). At 3.5 kbar the gradual increase in resistivity was observed below about 10 K in both salts, indicating the transition from a high-temperature metallic state to a low-temperature SDW state. According to the previous NMR results of the Ga salt,¹⁸ the SDW is incommensurate with the underlying lattice. Therefore, the optimum nesting vector of the Q1D Fermi surface is not commensurate but incommensurate with the underlying lattice.

The interlayer resistivity shows normal metallic behavior from room temperature down to low temperatures above the ICSDW transition, suggesting the coherent conduction along the least conducting direction. This behavior is in sharp contrast to that of TMTSF salts where the nonmetallic

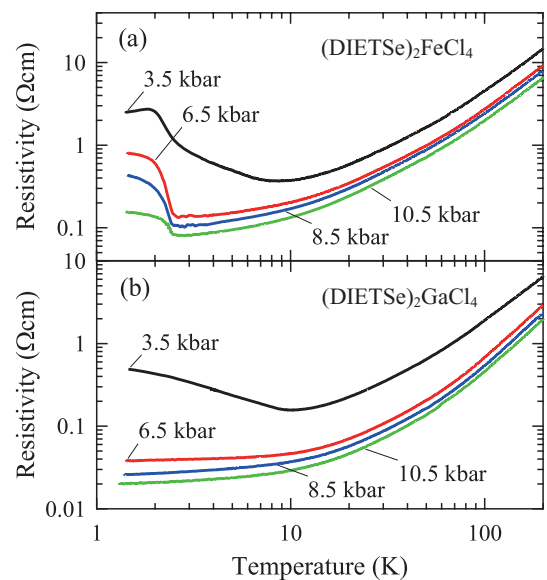


FIG. 2. (Color online) Temperature dependence of the interlayer resistivity of $(\text{DIETSe})_2\text{FeCl}_4$ (a) and $(\text{DIETSe})_2\text{GaCl}_4$ (b) under hydrostatic pressures.

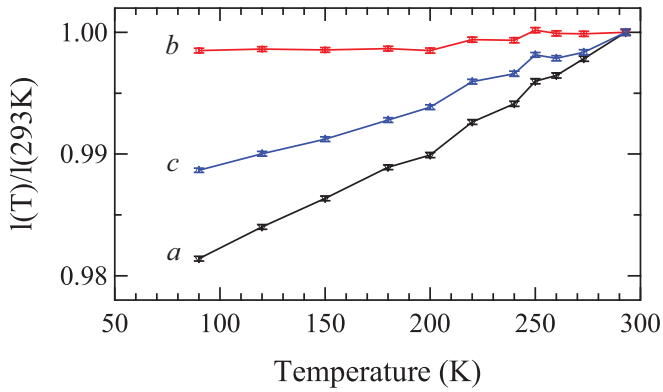


FIG. 3. (Color online) Temperature dependence of the normalized lattice constants of $(\text{DIETSe})_2\text{FeCl}_4$.

behaviors are observed in the interlayer resistivity at high temperatures and low pressures, indicating the incoherent transport.²² In $(\text{DIETSe})_2\text{MCl}_4$ [$M = \text{Fe}, \text{Ga}$], the so-called “iodine bond” works effectively to build the supramolecular-like structure.^{17,23} Actually, the short $\text{I} \cdots \text{Cl}$ contacts (3.50 and 3.51 Å for the Fe and Ga salts, respectively) exist between donor molecules and tetrahedral anions, which is about 6% shorter than the sum of the van der Waals radii (3.73 Å).¹⁷ Figure 3 shows the temperature dependence of the lattice constants of $(\text{DIETSe})_2\text{FeCl}_4$. The thermal expansion along the b -axis direction is very small compared with those of other axes. These experimental evidences indicate that the component molecules are closely packed along the b -axis direction due to the “iodine bond,” resulting in the coherent interlayer transport.

In accordance with the previous a -axis resistivity experiments,²⁰ the ICSDW transition is suppressed by applying the hydrostatic pressure in both salts as shown in Fig. 2. It suggests the suppression of nesting instability in Q1D Fermi surface due to increased Fermi-surface warping. The critical pressure P_c of ICSDW is about 5.5 kbar and 6.5 kbar for $(\text{DIETSe})_2\text{FeCl}_4$ and $(\text{DIETSe})_2\text{GaCl}_4$, respectively.²⁰ Above the P_c , $(\text{DIETSe})_2\text{GaCl}_4$ shows normal metallic behavior down to the lowest temperature of the experiment [Fig. 2(b)]. In contrast, $(\text{DIETSe})_2\text{FeCl}_4$ shows a rapid increase in the temperature dependence of resistance around 2.5 K even above P_c [Fig. 2(a)]. This is attributable to the AF transition of d -electron spins, because the magnetic anisotropy due to the onset of AF transition has been observed below this temperature.¹⁷ Since the d -electron spins are localized on Fe atoms, the AF order is most probably commensurate with the underlying lattice. The large increase in resistance below the AF transition implies the partial gap at the Fermi energy due to the formation of AF-induced commensurate SDW (CSDW). When the up and down spins of Fe^{3+} ($S = 5/2$) periodically alternate along the a axis, the $2k_F (= \pi/a)$ internal field appears. In this case, a Q1D metal become unstable through the π - d interaction. Therefore, the low temperature transport properties of $(\text{DIETSe})_2\text{FeCl}_4$ are ascribable to the interplay between the SDW instability of Q1D π electrons and the periodic local moments of AF d -electron spins.

At the low pressure below P_c , the original ICSDW and AF-induced CSDW are considered to coexist in the ground state

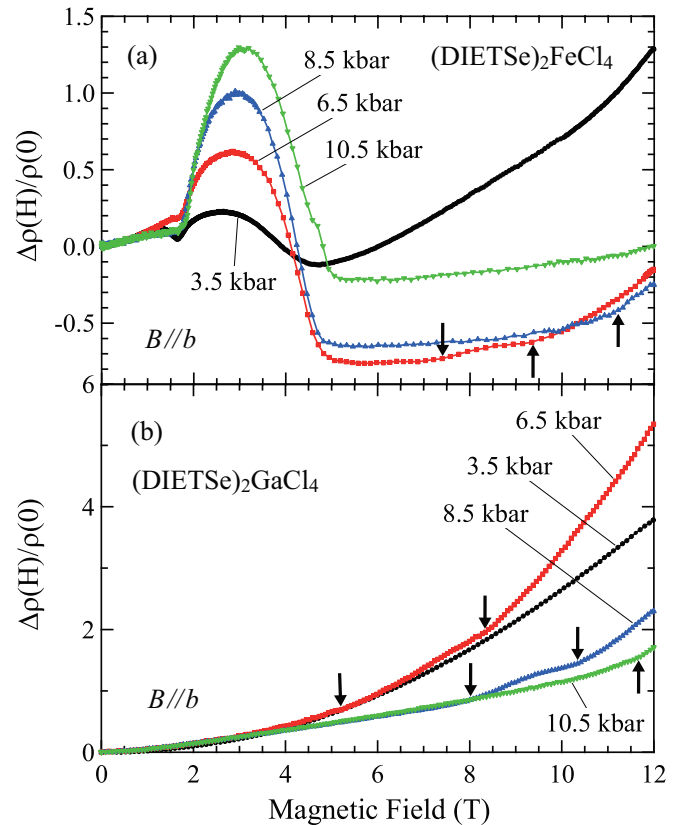


FIG. 4. (Color online) The interlayer longitudinal MR of $(\text{DIETSe})_2\text{FeCl}_4$ (a) and $(\text{DIETSe})_2\text{GaCl}_4$ (b) under the magnetic field along the b axis at 1.5 K. The arrows indicate the positions of kink which is defined by the peak in the second derivative of MR $d^2\rho/dH^2$, suggesting the FISDW transitions.

of $(\text{DIETSe})_2\text{FeCl}_4$. We note that the increase in resistivity below the ICSDW transition is not so large, implying the imperfect nesting of the Fermi surface. We speculate that the remaining, if any, Fermi surfaces below the ICSDW transition are further reconstructed by the commensurate AF potential, giving rise to the increase in resistivity below the AF transition in $(\text{DIETSe})_2\text{FeCl}_4$.

Figures 4(a) and 4(b) show the interlayer longitudinal MR of $(\text{DIETSe})_2\text{MCl}_4$ [$M = \text{Fe}, \text{Ga}$] under the magnetic field along the b axis at 1.5 K. The MR of $(\text{DIETSe})_2\text{FeCl}_4$ shows a steep change around 1.5 T. This is caused by a spin-flop transition of d -electron spins as confirmed by the magnetic torque measurement.²⁰ The resistance hump above the spin-flop field becomes larger with increasing pressure. The MR change, $\Delta\rho(H)/\rho(0) = [\rho(H) - \rho(0)]/\rho(0)$, reaches to 130% under the pressure of 10.5 kbar in $(\text{DIETSe})_2\text{FeCl}_4$. This is a clear indication of spin-charge coupling. The large resistance hump above the spin-flop field is suppressed around 5 T, which corresponds to the boundary between the canted AF state and the field-induced paramagnetic state. Actually, the magnetic moments of Fe^{3+} ($S = 5/2$) saturate around 5 T as confirmed by the magnetic torque measurement.²⁰ The $(\text{DIETSe})_2\text{GaCl}_4$ does not show such anomalous MR at low fields below 5 T as shown in Fig. 4(b), because of the absence of d -electron spins.

In the high magnetic field region above 5 T, the MR under 3.5 kbar is rather large for both salts because of the ICSDW ground state. On the other hand, under the high pressure of 10.5 kbar the MR above 5 T is rather small because of the metallic state. We note that the AF-induced gap should disappear at high magnetic fields above 5 T in $(\text{DIETSe})_2\text{FeCl}_4$ because of the field-induced paramagnetic state of d -electron spins.

In the intermediate pressure region above P_c , we observed the kink structures in the magnetic-field dependence of MR at high magnetic fields denoted by arrows in Figs. 4(a) and 4(b). The kink field was defined by the peak in the second derivative of MR, $d^2\rho/dH^2$. Such behavior is common to both salts, indicating the intrinsic properties of the Q1D π -electrons. These anomalies are reminiscent of a cascade of FISDW transitions. The temperature–pressure–magnetic-field phase diagrams of $(\text{DIETSe})_2\text{FeCl}_4$ and $(\text{DIETSe})_2\text{GaCl}_4$ are illustrated in Figs. 5(a) and 5(b), respectively. The previous results of the a -axis resistance are also involved in these phase diagrams.²⁰ The FISDW phase appears at high magnetic fields and high pressures above P_c . The critical field of FISDW increases with increasing pressure, as observed in the FISDW phases of TMTSF salts.⁹ Because the high pressure suppresses the nesting instability of the Q1D Fermi surface, a higher magnetic field is required to induce FISDW at a higher pressure. The observed behavior is consistent with the FISDW scenario. What is remarkable is the presence of AF order of d -electron spins which coexist with ICSDW below P_c in $(\text{DIETSe})_2\text{FeCl}_4$. The hydrostatic pressure suppresses the SDW instability, while the AF transition temperature and the critical field of the AF phase gradually increase with increasing pressure. The latter indicates the increase in the π - d interaction under pressure in $(\text{DIETSe})_2\text{FeCl}_4$. In order to precisely investigate these low temperature electronic states and spin-charge interaction, we have studied angle-dependent magnetoresistance as shown below.

A. Angle-dependent magnetoresistance: Lebed resonance

Figure 6(a) shows the angle-dependent MR of $(\text{DIETSe})_2\text{GaCl}_4$ at 1.5 K and 12 T under hydrostatic pressures up to 10.5 kbar. The magnetic field was rotated in the b - c plane, which is normal to the most conducting a axis. The angle θ is defined by the angle between the b axis and the magnetic field direction. The resistivity at 3.5 kbar is about one order of magnitude larger than those of the other pressures, and shows no notable anomalies in the angular dependence. It indicates the disappearance or reconstruction of the Q1D Fermi surface due to the ICSDW transition. In contrast, dip structures are clearly observed in MR around the b axis (0 and 180 degrees) at high pressures above 6.5 kbar.

Figure 6(b) shows the magnetic-field dependence of the angle-dependent MR of $(\text{DIETSe})_2\text{GaCl}_4$ at 10.5 kbar. The dip structures become clear with increasing magnetic field, although the positions of dips are independent of magnetic field strength. These results indicate that the observed dip structures are ascribed to the geometrical effects of Fermi surface. The positions of dips in MR are periodic in $\tan\theta$ as shown in Fig. 6(c). The fitted solid line in Fig. 6(c) is expressed as $\tan\theta = 0.37N$, where N represents integers

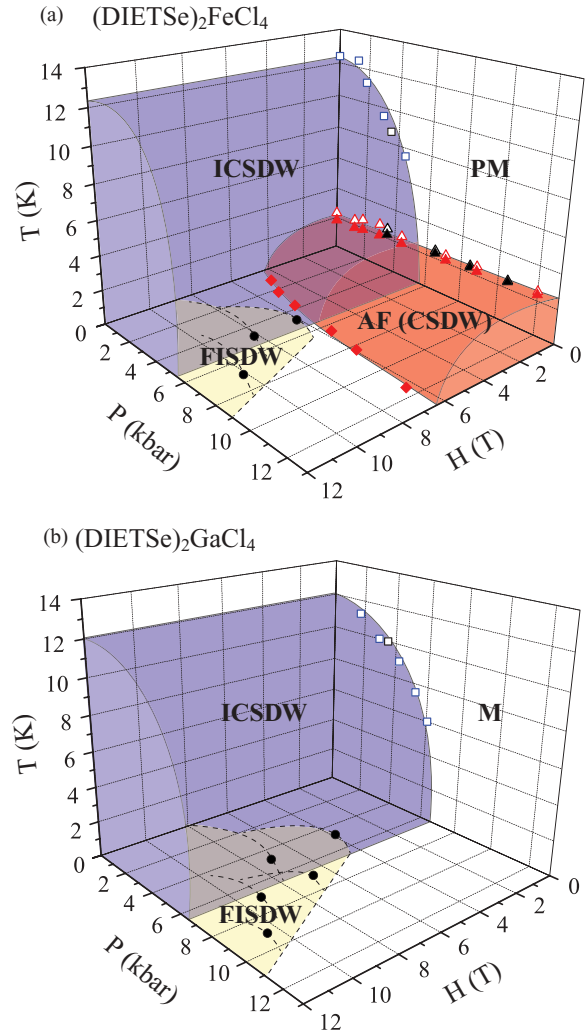


FIG. 5. (Color online) Temperature–pressure–magnetic-field phase diagrams of $(\text{DIETSe})_2\text{FeCl}_4$ (a) and $(\text{DIETSe})_2\text{GaCl}_4$ (b). Black symbols denote the present results of interlayer b -axis resistance at 1.5 K, while blue and red symbols represent the previous results of intralayer a -axis resistance at 0.6 K.²⁰ Open squares: the onset SDW transition temperature, where the resistivity shows a minimum. Open red triangles: onset AF transition temperature. Closed red triangles: the temperature where $d\ln(\rho)/d(1/T)$ shows a peak, corresponding to the long-range AF ordering temperature. Closed diamonds: phase boundary between the AF state and field-induced paramagnetic state, deduced from the offset of MR anomaly.²⁰ Closed circles: FISDW transitions defined by the peak in the second derivative of MR in Fig. 4. PM: paramagnetic metal. M: metal. The lines are guides to the eye.

($N = 0, \pm 1, \pm 2, \dots$). Since this compound is orthorhombic, the so-called Lebed resonance should appear at the magic angles:^{24–27}

$$\tan\theta = c/b \times N,$$

where c and b are the lattice constants along the c and b axis, respectively. The ratio of the lattice constants c/b of $(\text{DIETSe})_2M\text{Cl}_4$ [$M = \text{Fe}, \text{Ga}$] is 0.379 at room temperature.¹⁷ This value is very close to the observed one. Therefore, the angle-dependent MR oscillation (AMRO) is undoubtedly attributed to the Lebed resonance effect. Based on these

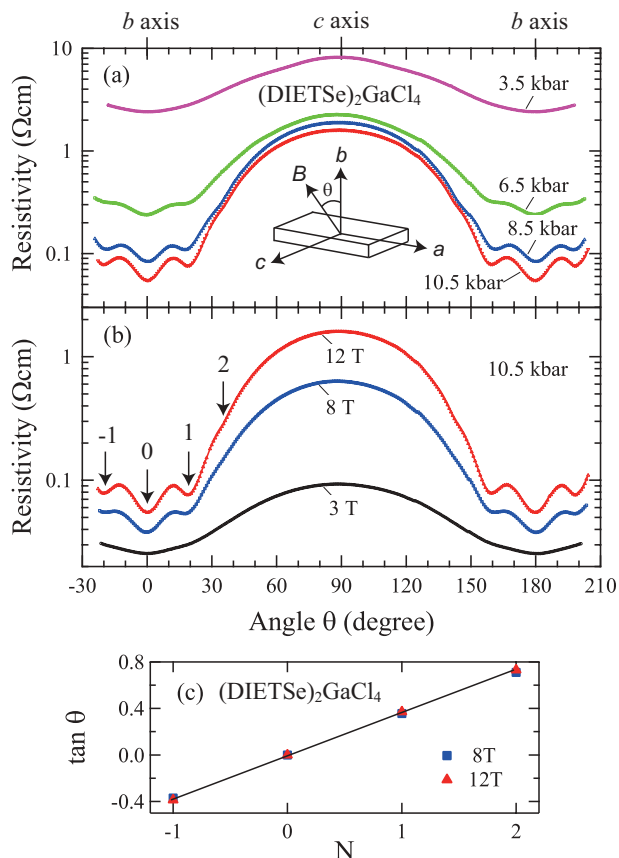


FIG. 6. (Color online) (a) Angular dependence of MR in (DIETSe)₂GaCl₄ at 1.5 K and 12 T under high pressures up to 10.5 kbar. (b) Magnetic field dependence of the angle-dependent MR under 10.5 kbar. (c) The positions of the dips in the MR plotted against $\tan \theta$.

experimental results, we confirmed the existence of the Q1D Fermi surface in the metallic state under high pressures in (DIETSe)₂GaCl₄. The similar AMRO is also observed in (DIETSe)₂FeCl₄ under high pressure and high magnetic field.

Figures 7(a) and 7(b) show the angle-dependent MR at 1.5 K under 6.5 kbar of (DIETSe)₂FeCl₄ in the (a) high- and (b) low-magnetic field regions, respectively. We note that the ICSDW is suppressed at this pressure as seen in Figs. 2(a) and 5(a). In addition, the AF phase can be collapsed by a strong magnetic field. Therefore, (DIETSe)₂FeCl₄ is regarded as a paramagnetic metal above 5 T at 1.5 K. Actually, we observed AMRO characteristic of the Q1D Fermi surface at 6 T as shown in Fig. 7(a). It is to be noted that further increase in magnetic field induces the FISDW phases. However, the AMRO is still observed in the FISDW state at 12 T. (DIETSe)₂GaCl₄ also showed AMRO in the FISDW state under the intermediate pressure region above P_c . These results are presumably ascribed to magnetic breakdown.²⁴ Under a strong magnetic field, an excited quasiparticle may move along an open orbit by tunneling across the SDW gap, giving rise to AMRO. A series of dip structures in Fig. 7(a) is quite similar to that of (DIETSe)₂GaCl₄. The dips appear at the magic angles described by $\tan \theta = 0.37 N$ as shown in Fig. 7(c). Therefore, the observed AMRO at high magnetic fields in (DIETSe)₂FeCl₄ is also attributed to the

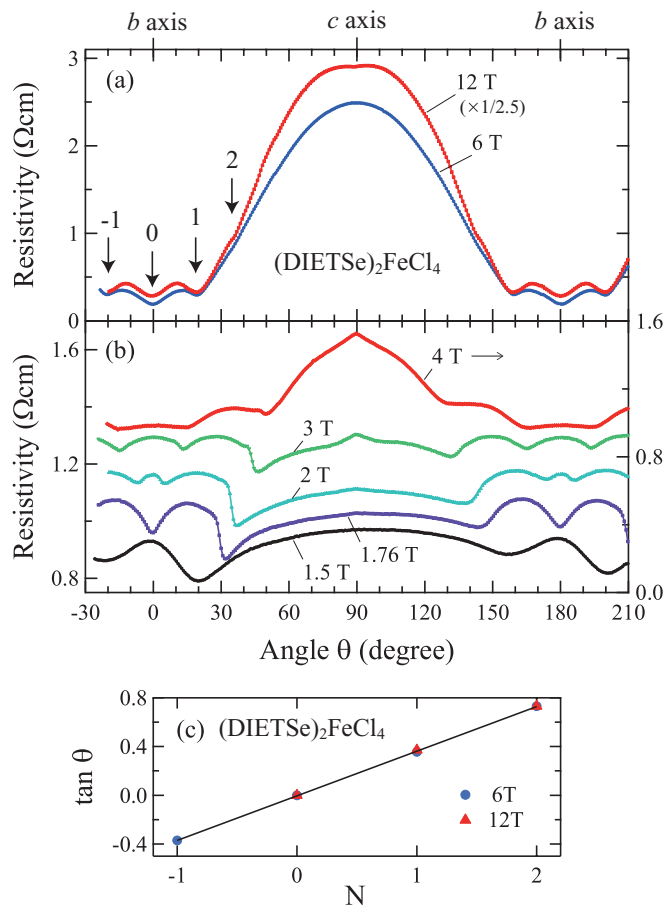


FIG. 7. (Color online) Angular dependence of MR in (DIETSe)₂FeCl₄ at 1.5 K under 6.5 kbar in the high magnetic field region (a) and the low magnetic field region (b). (c) The positions of the dips in the MR at 6 T and 12 T plotted against $\tan \theta$.

Lebed resonance effect. These results confirm that both salts have almost the same electronic states and Fermi surfaces with nesting instability. The hydrostatic pressure increases the warping of the Fermi surface, leading to the suppression of the ICSDW phase.

B. Hidden spin canting

At low magnetic fields below 4 T, a series of very anomalous MR is observed in (DIETSe)₂FeCl₄ as shown in Fig. 7(b). These anomalous angular dependences of MR are absent in (DIETSe)₂GaCl₄, and only observed in the low-field AF phase of (DIETSe)₂FeCl₄. Since the positions of these anomalies are strongly dependent on magnetic field strength, they are not ascribed to geometrical effects of Fermi surface. Actually, these low-field anomalies are seen both below P_c and above P_c regardless of Fermi surface. Figures 8(a) and 8(b) show the angle-dependent MR at the low pressure of 3.5 kbar below P_c . The Lebed resonance is absent in Figs. 8(a) and 8(b) because the salt is in the ICSDW state where the Q1D Fermi surface no longer exists. But the low-field anomalies are observed even below P_c .

As shown in Fig. 4(a), the resistivity of (DIETSe)₂FeCl₄ is very sensitive to the change in the magnetic structure of *d*-electron spins. The low-field anomalies in Figs. 7(b) and

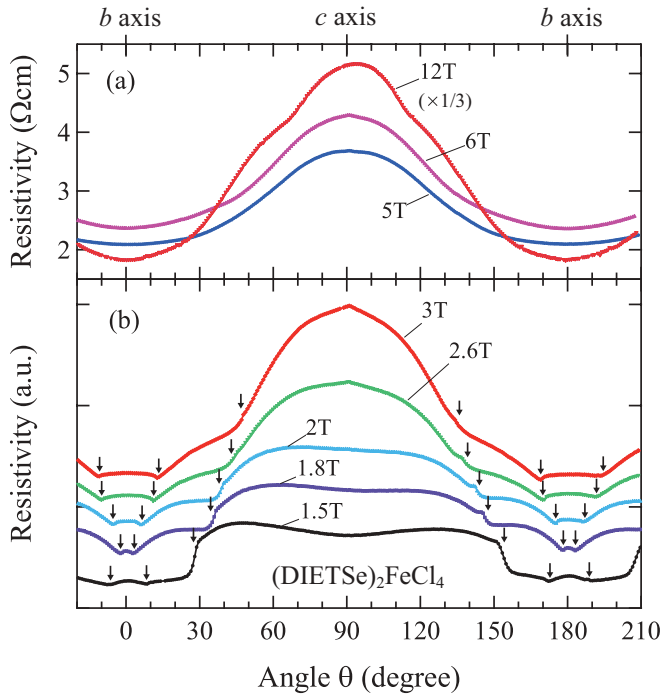


FIG. 8. (Color online) Angular dependence of MR in $(\text{DIETSe})_2\text{FeCl}_4$ at 1.5 K under 3.5 kbar in the high magnetic field region (a) and the low magnetic field region (b). The resistance minimum and the peak (or dip) in the derivative $d\rho/d\theta$ are indicated by arrows, corresponding to spin-flop transition.

8(b) are also related to the change in magnetic structure of d -electron spins. In order to demonstrate their magnetic-field direction and strength dependencies, we plotted the positions of anomalies in the polar plot [Fig. 9]. These anomalies are undoubtedly attributed to the spin-flop transition of d -electron spins, because the anomaly at 1.5 T along $H\parallel b$ corresponds to the spin flop as found in the magnetic torque experiment²⁰ and is connected continuously to other anomalies as shown in Fig. 9. We note that the spin-flop behavior is rather complicated and cannot be described by single-easy-axis antiferromagnet. Instead, the crystal is regarded as a two-easy-axes system

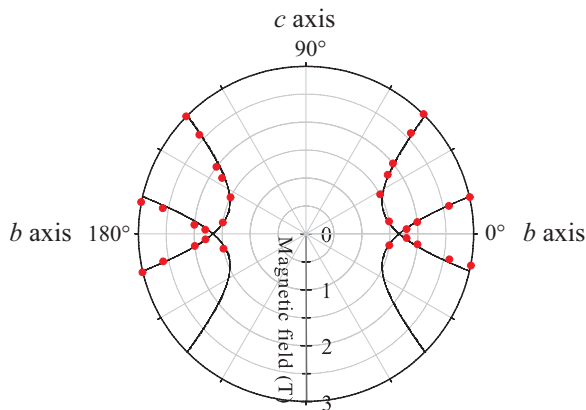


FIG. 9. (Color online) A polar plot of the anomalies in the angular dependence of MR of $(\text{DIETSe})_2\text{FeCl}_4$ at 1.5 K under 3.5 kbar. The closed symbols represent the points indicated by arrows in Fig. 7(b). Solid lines: the fit to experimental points using the hyperbola function.

whose oblique angle is tilted ± 16 degrees from the b axis towards the c axis because the positions of the spin flop are well described by the following critical hyperbola^{28,29} with two oblique angles $\theta = \pm 16$:

$$\frac{(H_b \cos \theta + H_c \sin \theta)^2}{A^2} - \frac{(-H_b \sin \theta + H_c \cos \theta)^2}{B^2} = 1,$$

where H_b and H_c denote the b - and c -axis component of external magnetic field, respectively. A and B are fitting parameters. The solid lines in Fig. 9 are fitted results using the values $A = 1.44$, $B = 0.95$, and $\theta = \pm 16$. Thus, we found the hidden spin canting³⁰⁻³⁶ in $(\text{DIETSe})_2\text{FeCl}_4$ from the magnetotransport measurements.

The observed hidden spin canting can be ascribed to single-ion anisotropy with preferential direction for magnetic moments located on different sublattice or Dzyaloshinsky-Moriya (DM) interaction, or both. Since there are two orientations of the $M\text{Cl}_4$ anion in the crystal, the spin easy axis of each orientation might differ from one another. Miyazaki *et al.* discussed the important role of single-ion anisotropy in $(\text{EDO-TTFBr}_2)_2\text{FeX}_4$ [$X = \text{Cl}, \text{Br}$] which has the similar crystal structure with the DIETSe salts.¹⁴ Since tetrahedral counter anions are slightly distorted in both DIETSe and EDO-TTFBr₂ salts, single-ion anisotropy should be taken into account for the origin of magnetic anisotropy in these compounds.

The spin flop of d -electron spins strongly alters the conductivity in $(\text{DIETSe})_2\text{FeCl}_4$, indicating the significant interplay between itinerant electrons and local moments. There are other π - d conductors exhibiting resistance change due to spin-flop transition.^{10-15,37} However, details of its angular dependence have not been reported except for β -(EDT-DSDTFVSDS)₂FeBr₄, where abnormal twin dip structures were observed in the angular dependence of MR.¹⁵ The origin of the abnormal behavior remains unsolved in β -(EDT-DSDTFVSDS)₂FeBr₄. In contrast, the anomalies in the angular dependence of MR in $(\text{DIETSe})_2\text{FeCl}_4$ are well explained by the hidden spin canting.

We also found clear hysteresis in the angular dependence of MR as shown in Fig. 10. The MR shows asymmetric behaviors with significant hysteresis near the spin-flop transition. The MR shows steep change at the outer phase boundary of the spin-flop transition, while the dip structures are seen at the inner (near the b axis) phase boundary of the spin-flop transition. The former manifests the strong first-order nature of the transition. The steplike steep change in resistance and associated hysteresis at the spin-flop transition becomes small with increasing magnetic field, indicating smearing of the spin-flop transition at high magnetic fields. They disappear above about 6 T as shown in Fig. 10(d), since the AF phase no longer exists. The hysteresis in MR may originate primarily from the presence of two easy axes and field-induced reconfigurations among magnetic domains or the movement of domain walls. In addition to quasiparticle scattering that would be influenced by such reconfigurations, we need to consider the possible interplay between the AF moments and ICSDW, because an ICSDW coexists with AF order in the ground state. We should take into account the internal degrees of freedom such as wave vectors, phases, and relative spin orientations of AF and SDW. The domain wall, if any, may also create a

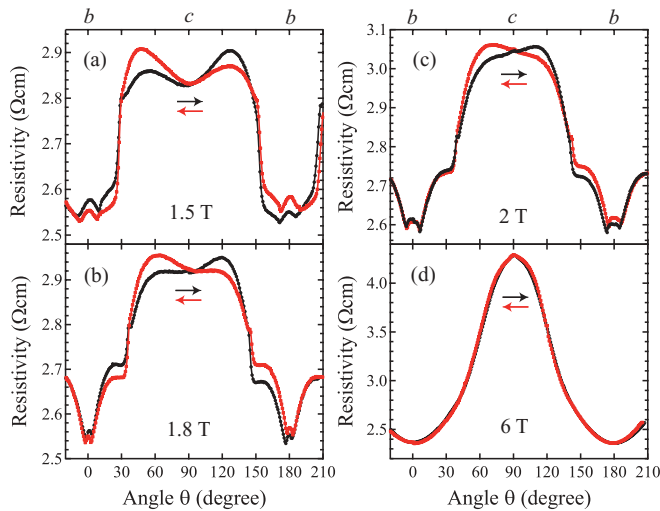


FIG. 10. (Color online) Hysteresis in the angular dependence of MR in $(\text{DIETSe})_2\text{FeCl}_4$ under 3.5 kbar at 1.5 T (a), 1.8 T (b), 2 T (c), and 6 T (d). The MR was measured at 1.5 K while rotating magnetic field forward (black points) and backward (red points) directions, respectively.

random potential that could contribute to the SDW pinning mechanism. Since there are many possible origins, further investigations are required to clarify the detailed mechanism of the anomalous MR behaviors.

IV. CONCLUSION

We have investigated magnetotransport behavior of the Q1D molecular conductor $(\text{DIETSe})_2\text{MCl}_4$ [$M = \text{Fe}, \text{Ga}$] under high pressure and high magnetic field. High pressure increases the warping of Fermi surface and therefore sup-

presses the ICSDW state. At high pressure and high magnetic field, the so-called Lebed resonance is observed in both salts. It indicates the existence of almost the same Q1D Fermi surface for both salts. Under the high pressure above P_c , some kink structures are observed in the magnetic-field dependence of MR at high magnetic fields, reminiscent of FISDW transition in both salts.

The AF order of d -electron spins coexists with the ICSDW at low pressure in $(\text{DIETSe})_2\text{FeCl}_4$ which shows a large change in resistance at the boundary of the AF phase. In addition, the quite anomalous MR is observed at the spin-flop field of d -electron spins. The MR change $\Delta\rho(H)/\rho(0)$ increases with increasing pressure, and reaches up to 130% at 10.5 kbar, indicating the significant interplay between itinerant electrons and local moments. The anomalies due to the spin-flop transition are also observed in the angle-dependent MR, associated with clear hysteresis. The positions of these anomalies in the polar plot are well described by the critical hyperbola with two oblique angles. Two magnetic easy axes are found to be tilted ± 16 degrees from the b axis towards the c axis. Thus, the presence of hidden spin canting has been uncovered by the transport measurements. These results demonstrate the highly susceptible nature of Q1D π electrons having an SDW instability against AF d -electron spins.

ACKNOWLEDGMENTS

This work was supported in part by Grants-in-Aid for the Global COE Program “International Center for Integrated Research and Advanced Education in Materials Science” and Scientific Research on Innovative Areas (20110006) from MEXT, Japan and a Grant-in-Aid for Young Scientists (B) (22740226) and Scientific Research (S) (23225005) from JSPS.

*Corresponding author: maesato@kuchem.kyoto-u.ac.jp

†Present address: Faculty of Agriculture, Meijyo University, 1-501 Shioyamaguchi, Tempaku-ku, Nagoya 468-8502, Japan.

‡Present address: Department of Applied Chemistry, Ehime University, 3 Bunkyo-cho, Matsuyama, Ehime 790-8577, Japan.

§Present address: Department of Materials Science and Technology, Nagaoka University of Technology, 1603-1 Kamitomioka, Nagaoka, Niigata 940-2188, Japan.

¹E. Coronado and P. Day, *Chem. Rev.* **104**, 5419 (2004).

²T. Enoki and A. Miyazaki, *Chem. Rev.* **104**, 5449 (2004).

³H. Kobayashi, H. B. Cui, and A. Kobayashi, *Chem. Rev.* **104**, 5265 (2004).

⁴T. Sugimoto, H. Fujiwara, S. Noguchi, and K. Murata, *Sci. Technol. Adv. Mater.* **10**, 024302 (2009).

⁵S. Uji, H. Shinagawa, T. Terashima, T. Yakabe, Y. Terai, M. Tokumoto, A. Kobayashi, H. Tanaka, and H. Kobayashi, *Nature (London)* **410**, 908 (2001).

⁶N. Hanasaki, H. Tajima, M. Matsuda, T. Naito, and T. Inabe, *Phys. Rev. B* **62**, 5839 (2000).

⁷A. W. Overhauser, *Phys. Rev. Lett.* **4**, 462 (1960).

⁸A. W. Overhauser, *Phys. Rev.* **128**, 1437 (1962).

⁹W. Kang, S. T. Hannahs, and P. M. Chaikin, *Phys. Rev. Lett.* **70**, 3091 (1993).

¹⁰K. Enomoto, J. Yamaura, A. Miyazaki, and T. Enoki, *Bull. Chem. Soc. Jpn.* **76**, 945 (2003).

¹¹K. Okabe, J. Yamaura, A. Miyazaki, and T. Enoki, *J. Phys. Soc. Jpn.* **74**, 1508 (2005).

¹²J. Nishijo, A. Miyazaki, and T. Enoki, *Inorg. Chem.* **44**, 2493 (2005).

¹³T. Enoki, K. Okabe, and A. Miyazaki, in *Multifunctional Conducting Molecular Materials*, edited by G. Saito, F. Wudl, R. C. Haddon, K. Tanigaki, T. Enoki, H. E. Katz, and M. Maesato (RSC Publishing, Cambridge, 2007), pp. 153–160.

¹⁴A. Miyazaki, H. Yamazaki, M. Aimatsu, T. Enoki, R. Watanabe, E. Ogura, Y. Kuwatani, and M. Iyoda, *Inorg. Chem.* **46**, 3353 (2007).

¹⁵T. Fujimoto, S. Yasuzuka, K. Yokogawa, H. Yoshino, T. Hayashi, H. Fujiwara, T. Sugimoto, and K. Murata, *J. Phys. Soc. Jpn.* **77**, 014704 (2008).

¹⁶T. Fujimoto, T. Hayashi, T. Sugimoto, H. Yoshino, and K. Murata, *J. Phys. Soc. Jpn.* **78**, 014710 (2009).

¹⁷T. Shirahata, M. Kibune, M. Maesato, T. Kawashima, G. Saito, and T. Imakubo, *J. Mater. Chem.* **16**, 3381 (2006).

- ¹⁸C. Michioka, Y. Itoh, K. Yoshimura, Y. Furushima, M. Maesato, G. Saito, T. Shirahata, M. Kibune, and T. Imakubo, *J. Phys.: Conf. Ser.* **150**, 042124 (2009).
- ¹⁹M. Maesato, T. Kawashima, G. Saito, T. Shirahata, M. Kibune, and T. Imakubo, *Mol. Cryst. Liq. Cryst.* **455**, 123 (2006).
- ²⁰M. Maesato, T. Kawashima, Y. Furushima, G. Saito, H. Kitagawa, T. Shirahata, M. Kibune, and T. Imakubo, *J. Am. Chem. Soc.* **134**, 17452 (2012).
- ²¹K. Murata, H. Yoshino, H. O. Yadav, Y. Honda, and N. Shirakawa, *Rev. Sci. Instrum.* **68**, 2490 (1997).
- ²²L. Degiorgi and D. Jerome, *J. Phys. Soc. Jpn.* **75**, 051004 (2006).
- ²³T. Imakubo, “*Fundamentals and applications of tetrathiafulvalene, halogenated tfs*”, in *TTF Chemistry*, edited by J. Yamada and T. Sugimoto (Kodansha and Springer, Tokyo, 2004), Chap. 3.
- ²⁴T. Osada, A. Kawasumi, S. Kagoshima, N. Miura, and G. Saito, *Phys. Rev. Lett.* **66**, 1525 (1991).
- ²⁵M. J. Naughton, O. H. Chung, M. Chaparala, X. Bu, and P. Coppens, *Phys. Rev. Lett.* **67**, 3712 (1991).
- ²⁶T. Osada, S. Kagoshima, and N. Miura, *Phys. Rev. B* **46**, 1812 (1992).
- ²⁷T. Osada and E. Ohmichi, *J. Phys. Soc. Jpn.* **75**, 051006 (2006).
- ²⁸C. J. Gorter and J. Haantjes, *Physica* **18**, 285 (1952).
- ²⁹T. Nagamiya, *Prog. Theor. Phys.* **11**, 309 (1954).
- ³⁰A. Herweijer, W. J. M. de Jonge, A. C. Botterman, A. L. M. Bongaarts, and J. A. Cowen, *Phys. Rev. B* **5**, 4618 (1972).
- ³¹K. Kopinga, Q. A. G. V. Vlimmeren, A. L. M. Bongaarts, and W. J. M. D. Jonge, *Physica B + C* **86-88**, 671 (1977).
- ³²J. A. J. Basten, Q. A. G. van Vlimmeren, and W. J. M. de Jonge, *Phys. Rev. B* **18**, 2179 (1978).
- ³³D. W. Engelfriet, W. L. Groeneveld, H. A. Groenendijk, J. J. Smit, and G. M. Na, *Z. Naturforsch. Teil A* **35**, 115 (1980).
- ³⁴R. L. Carlin, K. O. Joung, A. van der Bilt, H. den Adel, C. J. O’Connor, and E. Sinn, *J. Chem. Phys.* **75**, 431 (1981).
- ³⁵Y.-Q. Tian, C.-X. Cai, X.-M. Ren, C.-Y. Duan, Y. Xu, S. Gao, and X.-Z. You, *Chem. Eur. J.* **9**, 5673 (2003).
- ³⁶X.-Y. Wang, L. Wang, Z.-M. Wang, G. Su, and S. Gao, *Chem. Mater.* **17**, 6369 (2005).
- ³⁷T. Hayashi, X. Xiao, H. Fujiwara, T. Sugimoto, H. Nakazumi, S. Noguchi, T. Fujimoto, S. Yasuzuka, H. Yoshino, K. Murata, T. Mori, and H. Aruga-Katori, *J. Am. Chem. Soc.* **128**, 11746 (2006).